Influence of Nozzle Asymmetry on Supersonic Jets

R. W. Wlezien* and V. Kibens†
McDonnell Douglas Research Laboratories, St. Louis, Missouri

The flowfield and noise-generation charactaristics of jets from a series of nonaxisymmetric nozzles have been investigated at supersonic pressure ratios. Detailed acoustic measurements have revealed a strong azimuthal variation in the far-field components of screech and mixing noise. A phase-conditioned schlieren technique has been used to determine the screech modes and the characteristics of the time-mean flowfield. A variety of flow properties has been revealed, including mean jet vectoring, spreading enhancement, and screech suppression. A two-dimensional screech mode has been observed in contrast with the toroidal and helical modes of the reference jet.

Introduction

MODIFICATION of nozzle geometry by introduction of azimuthal asymmetry is a technique for controlling development of high-speed jets. Applications of this technique include thrust vectoring, mixing enhancement, and noise reduction. A series of nonaxisymmetric nozzles with azimuthally varying lip position has been investigated for the control of subsonic jets.[1,2] The supersonic performance of these nozzles is discussed in this paper.

The dynamics of supersonic jets with imbedded shocks and high-amplitude pure-tone screech have been studied by a number of investigators since the pioneering work of Powell.[3] Several noise-control techniques involving the use of tabs and baffles have been investigated. Norum[4] tested a variety of asymmetric nozzles and had some success in alleviating the screech feedback loop. Krothapalli et al.[5] clarified the relevant mechanisms in low-aspect-ratio rectangular jets. Phase-averaging techniques were used by Yu and Seiner[6] to determine the instability modes of axisymmetric jets. The present level of understanding of supersonic axisymmetric jets is detailed in the review by Seiner.[7]

This study was directed at both the gross flowfield characteristics and the modes and magnitudes of screech instabilities in supersonic jets from asymmetric nozzles. A detailed mapping of the acoustic far field was obtained from anechoic chamber tests. Phase-conditioned flow visualization techniques were used to clarify jet instability modes and the mean flowfield. The noise measurements are explained in the context of the visualization results, and a phenomenological grouping is used to categorize broadly the variety of observations.

Experimental Approach

Nozzle Geometry

The series of nozzle configurations is illustrated in Fig. 1. The reference axisymmetric nozzle A consists of the convergent termination of the flow-system contraction. The nonaxisymmetric nozzles are constant-diameter tubes with various cutout exit shapes. The inclined nozzles with lip extensions of 1 and 2 diam (D) are designated D and E, respectively. The tabbed nozzles have 1-diam lip extensions with 1, 2, 4, and 8 tabs and are designated G, N, P, and R. The jet origin is defined as the average axial position of the nozzle lip, as indicated by the dashed circles. The azimuth angle ψ is referenced to the point on the nozzle farthest downstream for the inclined nozzles and the center of a tab for the tabbed nozzles. The constant-diameter portion of the nozzles is 2.5D in length from the plenum-chamber contraction to the jet

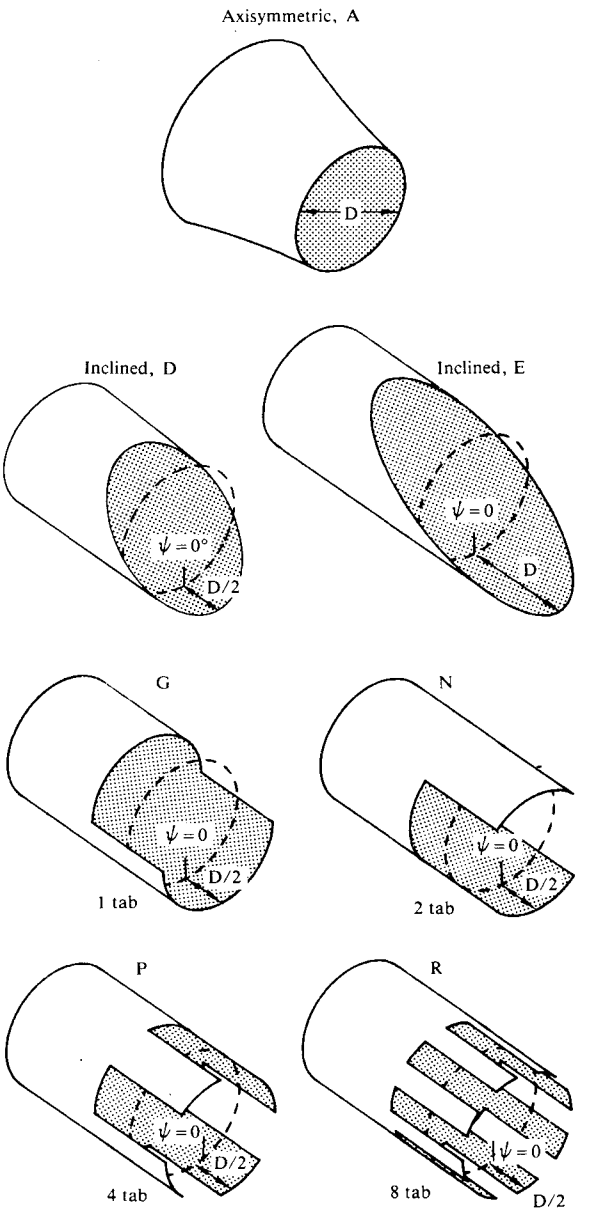

Fig. 1 Nozzle configurations.

Presented as Paper 86-0277 at the AIAA 24th Aerospace Sciences Meeting, Reno, NV, Jan. 6–9, 1986; received Aug. 21, 1986; revision received May 12, 1987.

*Scientist, Senior Member AIAA.
†Principal Scientist, Associate Fellow AIAA.

origin. This arrangement assures that the boundary-layer thickness is the same for all asymmetric nozzle configurations. Nozzles with internal diameters of 25.4 and 63.5 mm were used for the flow-visualization and acoustic tests, respectively.

Facilities

The flow visualization was conducted in an unlined test cell and employed the flow system shown in Fig. 2. Dry, unheated air from large storage bottles was supplied through primary and vernier control valves. The air was passed through a high-capacity muffler, a series of clean corners with turning vanes, a settling chamber with honeycomb and screens, and a 23 : 1 area ratio bicubic contraction to provide a stable, quiet flow source. A secondary contraction was used with the 25.4-mm nozzles. The nozzles were supported by an indexing adapter which allowed them to be rotated to arbitrary azimuths.

The plenum section and nozzles were installed in the Douglas Aircraft Co. Anechoic Acoustic Test Facility for the far-field noise measurements (Fig. 3). A constant-pressure servo-controlled valve system insured stability of the nozzle pressure ratio over the duration of a run. A novel three-dimensional microphone traversing system was used to characterize the azimuthal variation of the far-field noise. The traversing system provided horizontal motion by a rail-mounted carriage near the chamber ceiling, and vertical motion with an extendable boom. The microphone was mounted from a two-degree-of-freedom wrist to provide pointing capability. The traversing system was controlled by imbedded microprocessors which could be programmed with a predetermined schedule of measurement positions.

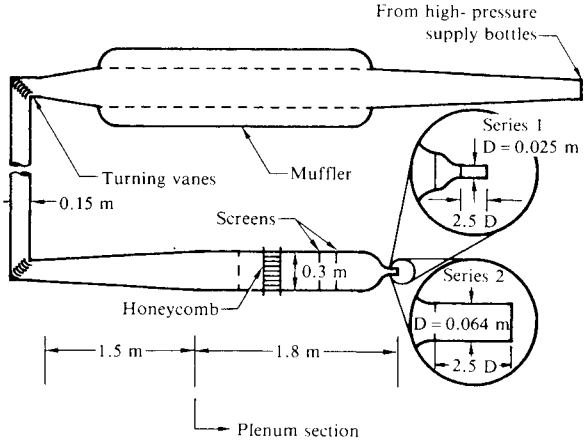

Fig. 2 Flow facility used for jet visualization; plenum section also used for acoustic test.

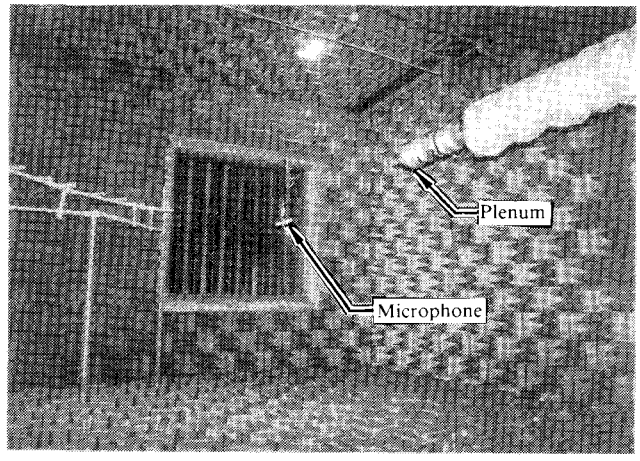

Fig. 3 Acoustic measurement configuration in anechoic chamber.

Acoustic-Test Instrumentation

Two B&K 6.35-mm microphones were suspended from the traverse to provide measurement redundancy. A hemisperical matrix of test points at a radius of $48D$ from the jet origin was used with 30 deg increments of azimuth ψ and elevation ϕ (Fig. 4); the microphones always pointed toward the jet origin. The physical constraints of the facility and traverse limited acquisition of data to a 90 deg range in ψ; the nozzle was manually rotated between quadrants to obtain a complete data set. The range of ψ was chosen to be 180 deg for nozzles D, E, G and N and 90 deg for nozzles A, P and R because of their inherent symmetry.

A PDP 11/70 minicomputer was used to acquire and process the data generated by the experiment. Mass flux, total temperature, and total pressure were monitored at each test point. A dedicated analyzer measured the one-third-octave spectra for each microphone. The spectra were transferred to the computer and corrected for microphone pressure response and free-field incidence; the data were compensated to standard day conditions; and pink noise and piston phone calibrations were conducted. The spectra were numerically integrated to determine the overall sound-pressure level (OASPL).

Phase-Conditioned Flow Visualization

A phase-conditioned schlieren system similar to those in Refs. 5–7 was developed to acquire visualization images that were phase-locked to the discrete screech tones generated by the jet. A conditionally triggered strobe light provided the schlieren light source, and both video and film photography were used to record the images.

The phase-conditioning system is illustrated in Fig. 5. A microphone placed near the flow acquired the screech synchronization signal, and a narrow-band filter eliminated unwanted spectral components. A comparator adjusted to detect zero crossings produced the pulse train designated as "screech trigger" in Fig. 5.

The schlieren light source did not have sufficient recovery time to respond directly to the trigger signal. Furthermore, multiple flashes of the strobe during a given video scan degraded the quality of the video record; therefore, the pulsed schlieren system was locked to the video system to provide one pulse per video field. A sync pulse derived from the video camera flagged the initiation of a video field at the rate of

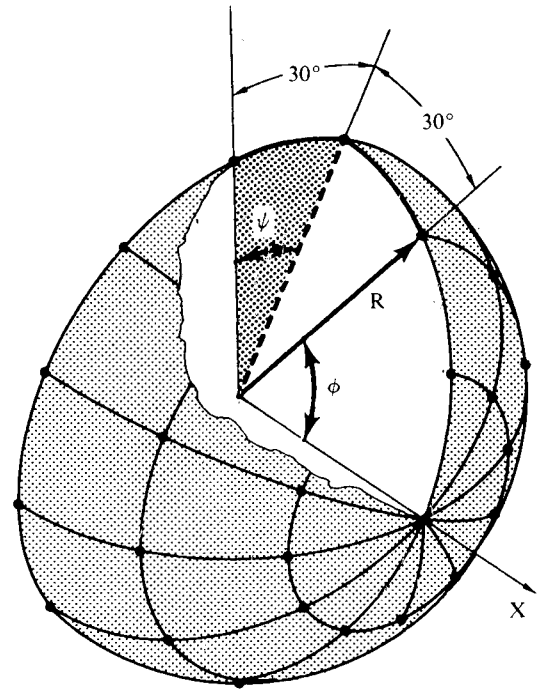

Fig. 4 Hemispherical grid of microphone positions.

60/s. The strobe was triggered on the leading edge of the first screech pulse after the video sync pulse. This event occurred very near the initiation of a field because the screech frequency was one to two orders of magnitude higher than 60 Hz. Although the flash duration was only 20 ns, the persistence of the video camera was sufficient to hold an image during an entire video field. A variable delay consisting of a 384-stage shift register with a continuously variable clock frequency allowed the light source to be flashed at an arbitrary phase of the screech cycle. A sequence of video images, acquired by slowly increasing the phase, effectively produced a slow-motion record of the jet unsteadiness that was phased to the screech tone.

The photographs appearing in this paper were obtained by optically averaging the phase-conditioned schlieren images by use of a standard 35-mm camera and black-and-white film. A 1-s exposure produced an average of 60-images on a single negative. The effect of the averaging is to de-emphasize the small-scale turbulence and enhance the flow characteristics phased to the screech.

Results

Acoustic Tests

The azimuthal variation of the far-field OASPL at a nozzle pressure ratio (NPR) of 2.8 and $\phi = 90$ deg is summarized in Fig. 6. At this pressure ratio all the nonaxisymmetric nozzles have OASPL levels at least 6 dB below that of the reference nozzle. Axisymmetric nozzle spectra show that the OASPL is dominated by the sharp peak characteristic of screech. Spectra for the nonaxisymmetric nozzles do not have similar peaks, presumably because the asymmetry of the nozzle lip and the resulting asymmetric shock structure effectively destroy the feedback system that supports the screech mode, as observed by Norum.[4] The azimuthal variation of the OASPL is no more than 1.5 dB, which is comparatively small and can be attributed to asymmetry of the mean flow.

The noise-generation characteristics of the nonaxisymmetric nozzles change radically at NPR = 4 (Fig. 7). The OASPL at $\phi = 90$ deg is strongly dependent on azimuth and nozzle configuration, with the inclined and 2-tab nozzles producing significant noise suppression at some angles, and augmentation at others. On the other hand, the 1- and 4-tab nozzles exhibit weak azimuthal variation similar to that at NPR = 2.8.

Figure 8a, the spectrum for the axisymmetric jet, has a dominant screech peak as observed at the lower NPR. When displayed as a shaded contour plot (Fig. 8b), this peak is represented as a light-toned vertical band. Contour plots for the inclined and 2-tab nozzles (Figs. 8c and 8d, respectively) demonstrate that azimuthal OASPL variation at $\phi = 90$ deg can be attributed primarily to a variation in screech amplitude. The screech band for the inclined nozzle is concentrated near $\psi = 90$ deg, the location of maximum OASPL in Fig. 7.

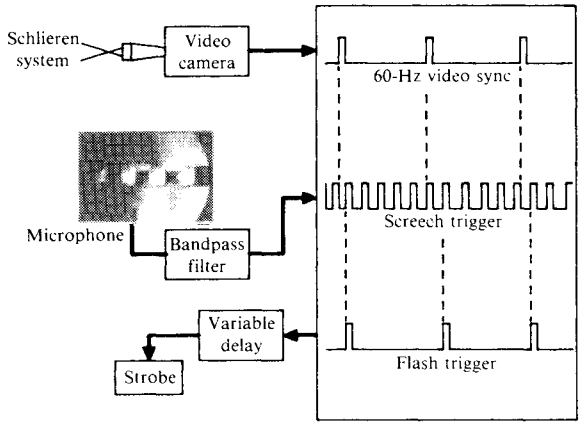

Fig. 5 Phase-conditioned schlieren video system.

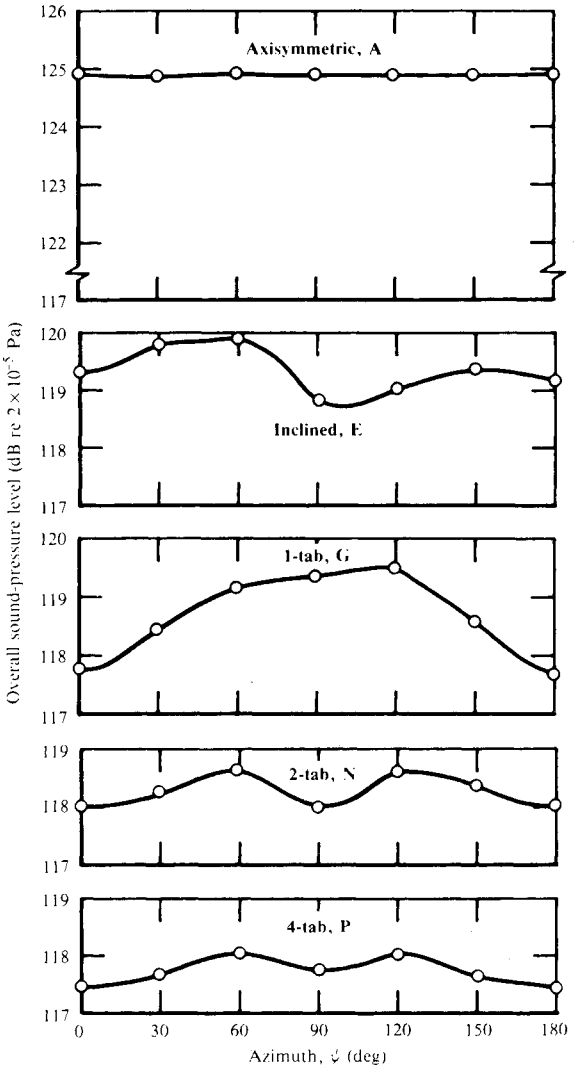

Fig. 6 Variation of OASPL at 48*D*; $\phi = 90$ deg, NPR = 2.8.

Similarly, the screech band for the 2-tab nozzle is located primarily near $\psi = 0$ and 180 deg. On the basis of these acoustic measurements, it is plausible that similar mechanisms are engaged in both cases.

The $\phi = 30$ deg OASPL data, which are dominated by mixing noise in the axisymmetric jet, are shown in Fig. 9. The noise fields for all configurations have strong asymmetry, and only the 4-tab nozzle produces consistent noise suppression. The spectra for nozzles at this microphone elevation are not screech dominated; therefore, another mechanism must be responsible for the asymmetry of the acoustic field. The ψ-dependence of the OASPL can be explained by the asymmetric spreading and deflection characteristics of these jets as verified by the flow visualization.

Flow Visualization

Phase-conditioned flow visualization was used to clarify the role of the unsteady flowfield in the generation of the asymmetric acoustic field and to characterize the time-mean asymmetry of the jets. Because it is impractical to represent the entire phase sequence observed in the videotapes, only representative views of the phase-averaged photographs are included here.

Figure 10 allows comparison between flow visualization pictures of the toroidal and helical modes of the underexpanded axisymmetric jet. The pictures are very similar to those obtained by Seiner[7] for the A1 and B modes. In the toroidal mode, the instability takes the form of toroidal structures in the shear layer which convect downstream and inter-

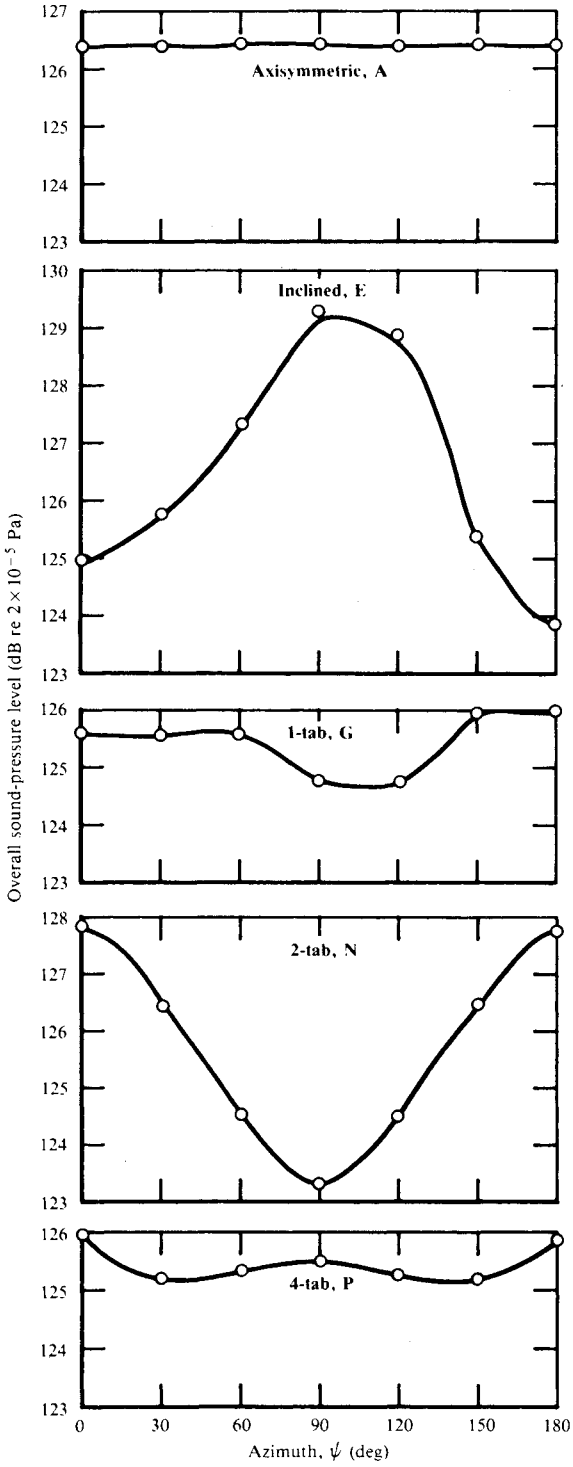

Fig. 7 Variation of OASPL at $48D$; $\phi = 90$ deg, NPR = 4.0.

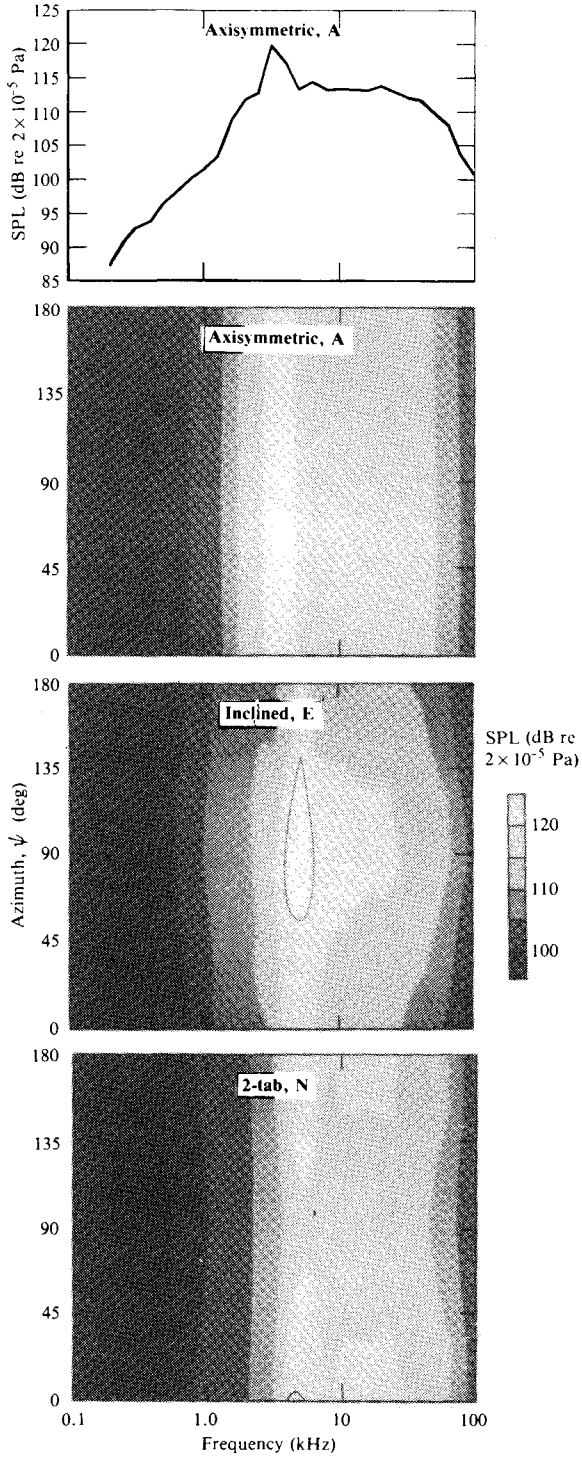

Fig. 8 Variation of acoustic spectra with azimuth at $48D$; $\phi = 90$ deg, NPR = 4.0.

act with the edges of the shock cells. The density perturbations associated with the toroids grow as they are convected downstream, but the attendant acoustic fronts are comparatively weak. The shock cells appear to be stationary during this process.

The helical mode, which exists for NPR > 2.3, is evident in the nonaxisymmetric acoustic field generated by the jet. The noise field generated by the NPR = 2.8 jet is 180 deg out of phase between the top and bottom of Fig. 10b. The videotape clearly shows a helical sound field which emanates from the vicinity of the third shock cell and propagates upstream and downstream. The third and subsequent shock cells are also displaced helically, as discussed by Yu and Seiner.[6] Visualization at other pressure ratios indicates that a similar mode persists at least to NPR = 4.0.

Typical phase-averaged photographs of the jets from inclined nozzles at NPR = 4.0 are shown in Fig. 11. The $\psi = 0$ views illustrate significant differences in the development of the jets. For nozzles with shallow exit-plane inclinations ($\leq$ that of nozzle D) the jet primarily deflects from the axis. As inclination is increased, the deflection becomes less predominant, and the jet diverges. The $\psi = 90$ deg views show a simultaneous contraction in the other direction. The degree of deflection and divergence generally increases with NPR. Divergence is also accompanied by a rearrangement of the shock

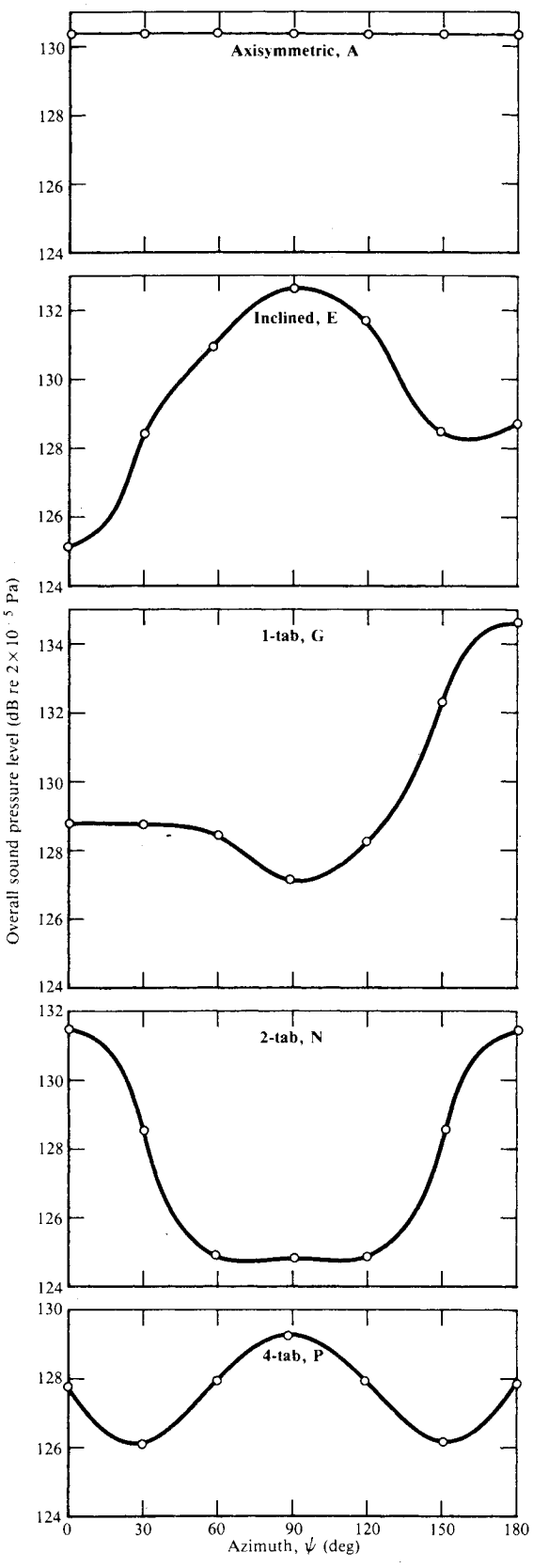

Fig. 9 Variation of OASPL at 48D; $\phi = 30$ deg, NPR = 4.0.

cells into a nonaxisymmetric configuration similar to the rectangular shock-cell geometry in a rectangular jet.[5]

Small deflection angles generally occur at low NPR or at high NPR when the nozzle inclination is large. In these cases, the Mach angle is such that the initial expansion intersects the extended portion of the nozzle and reflects as a shock. Jet deflection occurs for greater Mach angles relative to the nozzle inclination angle, where the initial expansion intersects the shear layer downstream of the end of the nozzle.

The results for the 1-tab nozzle (Fig. 12) are significant because the jet is deflected without appreciable spreading. The shock-cell structure is much more difficult to characterize from the schlieren visualization because it is more three-dimensional. Of the nozzles tested, the 1-tab nozzle produces the most efficient thrust vectoring. Nozzles with shorter and longer tabs exhibit characteristics similar to those of the inclined nozzles: the jets from long-tab nozzles diverge, and those from short-tab nozzles deflect. The divergence and deflection of the inclined and single-tab jets are shown as a function of NPR in Fig. 13.

Flow visualization pictures of the multi-tab nozzles are shown in Fig. 14. The symmetry of the cut-outs on the nozzles prevents net deflections of the jets. The 2-tab nozzle generates a divergent flow similar to that of the inclined nozzles, although the internal shock pattern is significantly different. The 4- and 6-tab nozzles produce jets with shock patterns similar to the reference jet. The spaces between the tabs provide an expansion path for the flow inside the nozzles and generate the rapidly spreading flow boundary that originates from the roots of the tabs. The pressure-relief mechanism also changes the structure of the shock-cell system, thus reducing the spacing relative to that of the reference jet at the same pressure ratio.

The phase-averaged visualization indicates the mechanism responsible for generating the asymmetric screech that was detected in the acoustic data for the inclined and 2-tab nozzles. In Fig. 11, the $\psi = 0$ view shows no evidence of a sound field, and on the videotape the shock fronts appear stationary in time. The $\psi = 90$ deg view shows an asymmetric acoustic field that is similar to the helical mode of the refer-

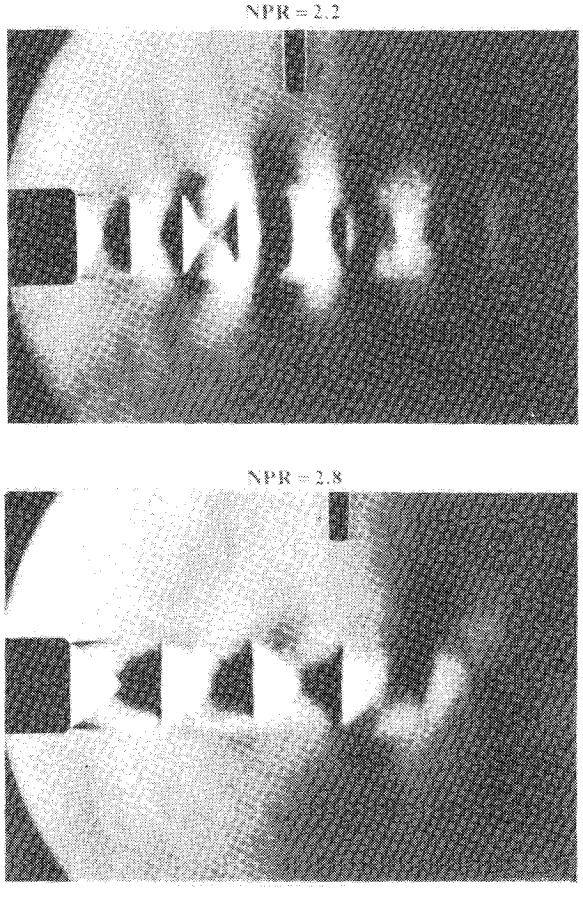

Fig. 10 Phase-averaged visualization of axisymmetric jet configuration A.

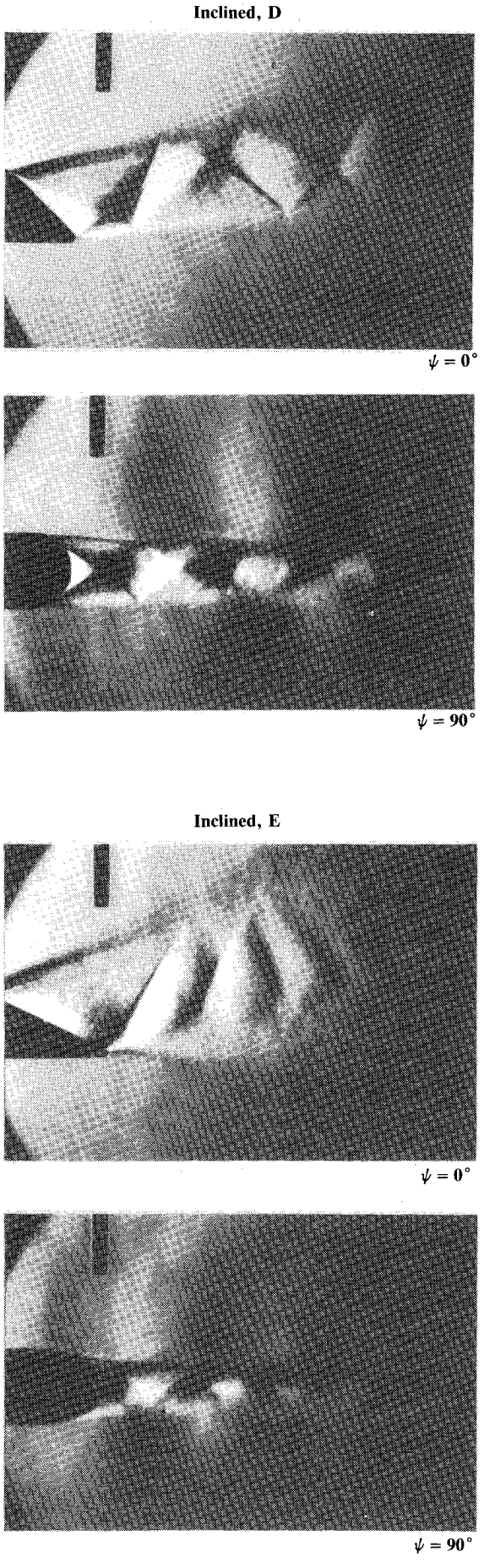

Fig. 11 Phase-averaged visualization of jets from inclined nozzles; NPR = 4.0.

ence jet. Taken together, these views indicate that the shock system oscillates in a lateral or flapping mode. Periodic shock-cell motion can be observed in the $\psi = 90$ deg view, and the far-field spectra show that the screech tone propagates primarily in a direction normal to the divergence plane. The visualization for the 2-tab nozzle shows similar characteristics in the $\psi = 0$ deg view. The lateral screech mode for these jets is very similar to that for jets from rectangular nozzles (see Ref. 5).

The data at $\phi = 30$ deg is dominated by mixing noise; the measured asymmetry can be explained by the asymmetric spreading and deflection of the jets. In the case of the 1-tab nozzle, the most intense noise was detected in the direction of jet deflection. For the jets that diverge, the greatest OASPL was recorded where the microphone was exposed to the great-

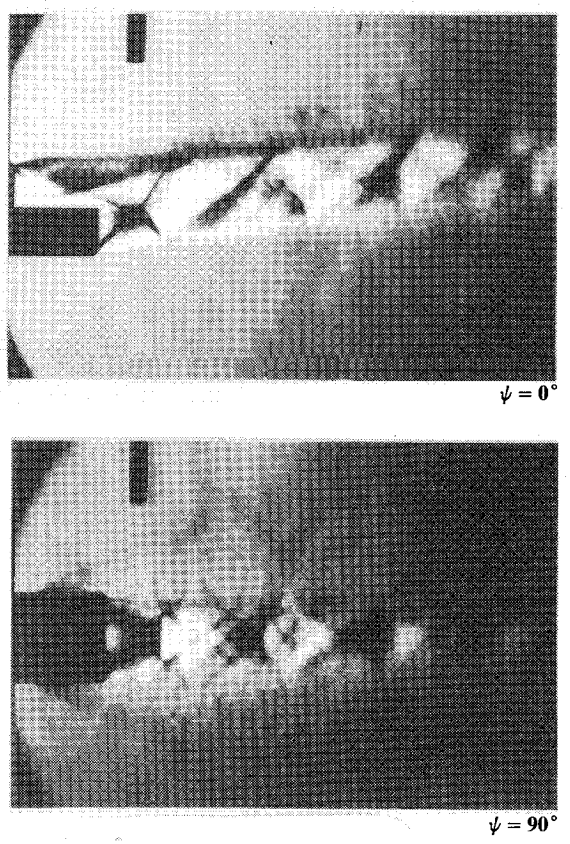

Fig. 12 Phase-averaged visualization of jet from 1-tab nozzle G; NPR = 4.0.

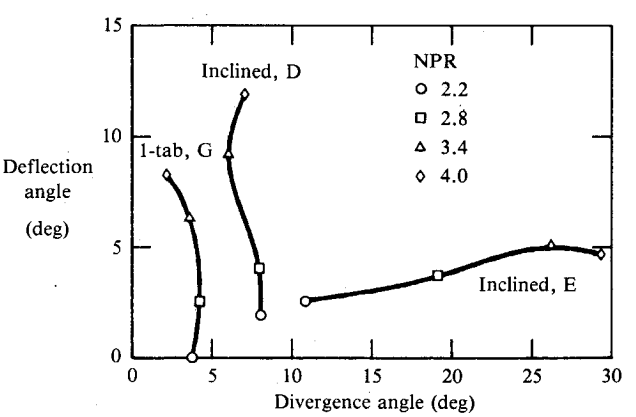

Fig. 13 Deflection and divergence of jets from inclined and 1-tab nozzles.

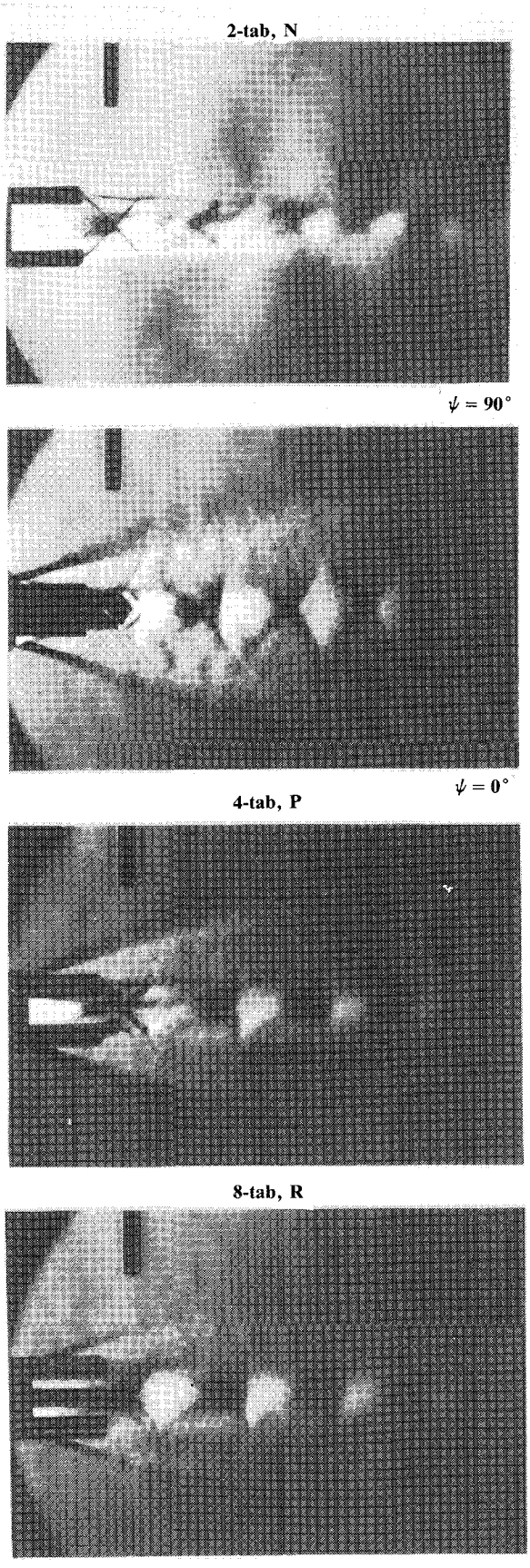

Fig. 14 Phase-averaged visualization of jet from multiple-tab nozzles; NPR = 4.0.

est portion of the shear layer. The 4- and 8-tab nozzles decrease the velocity of the jet through the initial expansion and appear to reduce noise because the jet has a lower overall velocity.

Conclusions

Supersonic jets from nonaxisymmetric nozzles exhibit a wider range of acoustic and flow properties than does an axisymmetric reference nozzle. Mean flow-properties such as deflection and divergence can be controlled to provide directional thrust or enhanced mixing. Dynamic shock oscillations can be controlled or eliminated, thereby alleviating the screech-tone generation. The characteristics of the observed flows can be organized into the following classes.

1) Axisymmetric: The reference jet undergoes at least two types of screech for NPR ≤ 4.0. At low supersonic NPR's, interaction between toroidal disturbances and the shock-cell structure is responsible for the first screech mode. At increased NPR's, the shock structure oscillates in a helical pattern, generating an asymmetric acoustic field from the third and subsequent shock cells.

2) Deflected: Short 1-tab and inclined nozzles generate jets that deflect with no appreciable change in spreading compared to the reference jet. The deflected jets have a complicated three-dimensional shock structure that does not support screech modes.

3) Divergent: Long 1-tab nozzles, inclined nozzles, and 2-tab nozzles produce jets that spread in one direction and contract in the other. It is likely that these jets increase mixing because of the augmented shear-layer surface area. At sufficiently high NPR's these jets experience a two-dimensional screech instability. Tonal screech noise and broadband mixing noise are generally suppressed in the plane of divergence and are increased in other directions.

4) Pressure-relieved: Multiple-tab nozzles release internal pressure before the jet reaches the ends of the tabs. The plume spreads faster than the reference jet, has a lower core-flow Mach number, and does not support screech.

This investigation has touched upon only a few aspects of flows from nonaxisymmetric nozzles. It is clear that many parameters govern the flow and noise fields and that relatively small changes in geometry or flow conditions can produce large, seemingly unpredictable variations in thrust, mixing, and noise. Further investigation of the detailed characteristics of these flows can lead to improved design of nonaxisymmetric nozzles.

Acknowledgment

This work was performed under the McDonnell Douglas Independent Research and Development program.

References

[1] Wlezien, R.W. and Kibens, V., "Passive Control of Jets with Indeterminate Origins," AIAA Paper 84-2299, 1984.

[2] Kibens, V. and Wlezien, R.W., "Active Control of Jets from Indeterminate-Origin Nozzles," AIAA Paper 85-0542, 1985.

[3] Powell, A., "On the Mechanism of Choked Jet Noise," *Proceedings of the Physical Society of London*, Sec. B, Vol. 66, 1953, pp. 1039–1056.

[4] Norum, T.D., "Screech Suppression in Supersonic Jets," *AIAA Journal*, Vol. 20, Feb. 1983, pp. 235–240.

[5] Krothapalli, A., Baganoff, D., and Hsia, Y., "On the Mechanism of Screech Tone Generation in Underexpanded Rectangular Jets," AIAA Paper 83-0727, 1983.

[6] Yu, J.C. and Seiner, J.M., "Nearfield Observations of Tones Generated from Supersonic Jet Flows," AIAA Paper 83-0706, 1983.

[7] Seiner, J.M., "Advances in High Speed Jet Aeroacoustics," AIAA Paper 84-2275, 1984.